

Summary from the working group on “Diffraction and Vector Mesons” at DIS 2008

Marcella Capua¹, Monika Grothe², Dmitry Ivanov³, and Mikhail Kapishin⁴

1- Calabria University and INFN - Dept of Physics
Arcavacata di Rende (CS) - Italy - capua@cs.infn.it

2- University of Wisconsin, Madison - Department of Physics
1150 University Ave., Madison, WI 53706 - USA - monika.grothe@cern.ch

3- SIM, Novosibirsk, Russia

4- Joint Institute for Nuclear Research - Laboratory of High Energy Physics
Joliot Curie 6, 141980 Dubna, Russia - kapishin@mail.desy.de

The contributions at the DIS2008 workshop in the working group on Diffraction and Vector Mesons are summarised.

1 Introduction

In the 1960s, one of the mysteries of strong interactions was the enormous proliferation of strong interacting particles or hadrons, which in addition, exhibit a striking property: the more massive the particles, the higher their spin with a linear correlations between the square of the particle mass and its spin. In Regge Theory [2] this correlation is described in the complex angular momentum plane by linear Regge trajectories. In this phenomenological approach diffraction corresponds to the exchange of the Pomeron trajectory, which has the quantum numbers of the vacuum. Pomeron trajectory exchanges dominate at high energies and its parameters have been derived from fits to the data of soft hadron-hadron interactions [3].

The study of the hadronic structure performed at large centre-of-mass energies in $p\bar{p}$ collisions at the Tevatron and in deep inelastic ep scattering (DIS) at HERA offer unique way to understand diffraction in terms of Quantum Chromo-Dynamics (QCD)(see e.g. [4] and references therein). Within the QCD framework diffractive events can be interpreted as processes in which a colour singlet combination of partons is exchanged.

The structure of the colour singlet can be studied using a QCD approach based on the hard scattering collinear factorization theorem [5]. It states that the diffractive cross section is a product of diffractive proton parton distribution functions (DPDFs) and partonic hard scattering cross sections. DPDFs are universal for diffractive ep DIS processes (inclusive, dijet and charm production) and obey the DGLAP evolution equations. Their extraction from inclusive diffractive processes and application to the analysis of diffractive dijet and charm production provides a test of QCD factorisation. Moreover, dijet and charm production data, directly sensitive to the gluon density in the colour singlet, can help in constraining the DPDFs when included in global fits.

2 Diffraction in ep interactions

The H1 and ZEUS experiments at HERA study processes of electron-proton DIS, $ep \rightarrow eX$, where X is the hadronic final state. A considerable part of the DIS cross section ($\sim 10\%$) comes from diffractive processes which are characterized by the presence of a leading proton in the final state carrying most of the proton beam energy and by a large rapidity gap (LRG) in the forward (proton) direction.

Figure 1 shows a schematic diagram of the diffractive process $ep \rightarrow eXp$ together with the relevant kinematic variables: the photon virtuality, Q^2 , the photon-proton centre-of-mass energy, W , and the square of the four-momentum transfer at the proton vertex, t . Relevant kinematic variables in diffraction are the fraction of the proton longitudinal momentum carried by the exchanged colour singlet object, $x_{\mathbb{P}}$, and the fraction of the exchanged momentum carried by the quark coupling to the virtual photon, β .

In analogy with the structure function F_2 for inclusive DIS the cross section of diffractive ep scattering is parameterized in terms of the diffractive structure function $F_2^{D(4)}(\beta, Q^2, x_{\mathbb{P}}, t)$.

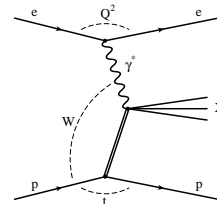


Figure 1: Diagram of the diffractive process $ep \rightarrow eXp$.

2.1 Inclusive and semi-inclusive diffraction in ep interactions

Diffractive processes at HERA are selected in several ways: by requiring the presence of a large rapidity gap (LRG method [6]), by observing a leading proton in the final state by means of a dedicated leading proton spectrometer (LP method [7]) or by studying the hadronic mass spectrum observed in the central detector (M_X method [8, 9]) to determine the diffractive contribution statistically.

The different methods treat in different ways the contribution of non-diffractive processes, like exchanges of the sub-leading Regge trajectories, and the background from proton dissociation processes.

The ZEUS experiment presented [18] the diffractive inclusive DIS results obtained with all the three experimental methods [10, 11], and their comparison to H1 recent results obtained with the LRG and LP methods [14, 15]. The results obtained with the three methods were compared in bins of M_X , Q^2 and $x_{\mathbb{P}}$ in terms of the diffractive reduced cross section, $\sigma_r^{D(4)}(\beta, Q^2, x_{\mathbb{P}}, t)$. The latter coincides with the diffractive structure function, $F_2^{D(4)}$, if the ratio of the cross sections for longitudinally and transversely polarised virtual photons is neglected. The reduced cross section $\sigma_r^{D(3)}(\beta, Q^2, x_{\mathbb{P}})$ is integrated over t for the LRG and M_X methods which do not allow a direct measurement of t , possible only with the LP method.

The LRG and LP results of ZEUS cover kinematic range: $Q^2 > 2 \text{ GeV}^2$, $M_X > 2 \text{ GeV}$, $40 < W < 240 \text{ GeV}$ and proton fractional momentum losses $0.0002 < x_{\mathbb{P}} < 0.02$ (LRG) or $0.0002 < x_{\mathbb{P}} < 0.1$ (LP). With the LRG and M_X methods high M_X values are not accessible. Events in which proton dissociates into a low mass state give contribution to the measured cross section. A detailed study of the events of proton dissociation allowed ZEUS to estimate their fraction in the LRG inclusive sample as $25 \pm 1(\text{stat.}) \pm 3(\text{syst.})\%$. In the LP method the proton dissociation background is negligible for $x_{\mathbb{P}} < 0.02$.

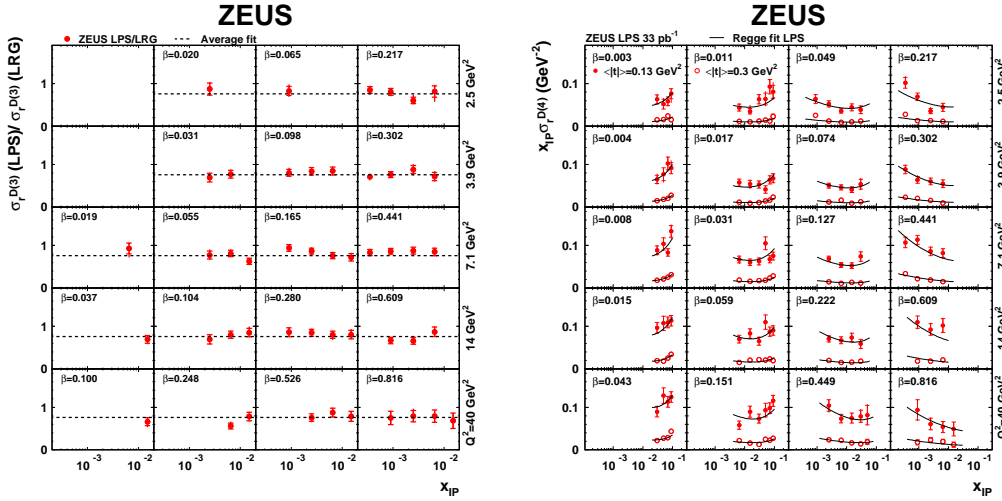


Figure 2: Ratio of the reduced diffractive cross sections obtained by ZEUS with the LP and the LRG methods as a function of x_{IP} for different values of Q^2 and β . (left). Reduced diffractive cross section obtained with the LP method measured in two t bins as a function of x_{IP} for different values of Q^2 and β (right). The data are compared with the results of a Regge fit.

The ratio of the reduced diffractive cross sections, $\sigma_r^{D(3)}$, obtained with the LP and LRG methods is found to be independent of Q^2 , x_{IP} and β (Fig. 2, left). A similar comparison has been performed by H1, also showing a good agreement [19].

The ZEUS experiment has also shown the first measurement, obtained with the LP method in two t bins, of the reduced cross section $\sigma_r^{D(4)}$ as a function of x_{IP} (Fig. 2, right). The results show the same x_{IP} dependence for each Q^2 and β bin. A Regge fit indicates that the shape of the x_{IP} dependence is the same in two t bins.

A satisfactory agreement between the data obtained with the LP method in both the ZEUS and H1 experiments has been observed. The ZEUS and H1 results are consistent with the hypothesis of proton vertex factorization [12]. Figure 3 (left) shows a reasonable agreement of the ZEUS results obtained with the M_X and LRG methods. The different x_{IP} dependence in some bins at low Q^2 may be ascribed to the contribution of the sub-leading Reggeon and pion trajectories which is suppressed in the M_X method and not suppressed in the LRG method. A comparison of the results obtained with the LRG method by ZEUS and the analogous results from H1, fig. 3 (right), shows a reasonable agreement.

The H1 Collaboration presented [20] the results on the diffractive PDFs [14], extracted from the H1 LRG inclusive measurements for $Q^2 > 8.5 \text{ GeV}^2$, $M_X \geq 2 \text{ GeV}$ and $\beta \leq 0.8$. The quark singlet and gluon distributions are extracted from NLO QCD fits to the data, the H1 2006 DPDF Fit A and B. These two fits differ in the parameterisation chosen for the gluon density at the starting scale for the QCD evolution. The resulting gluon distribution

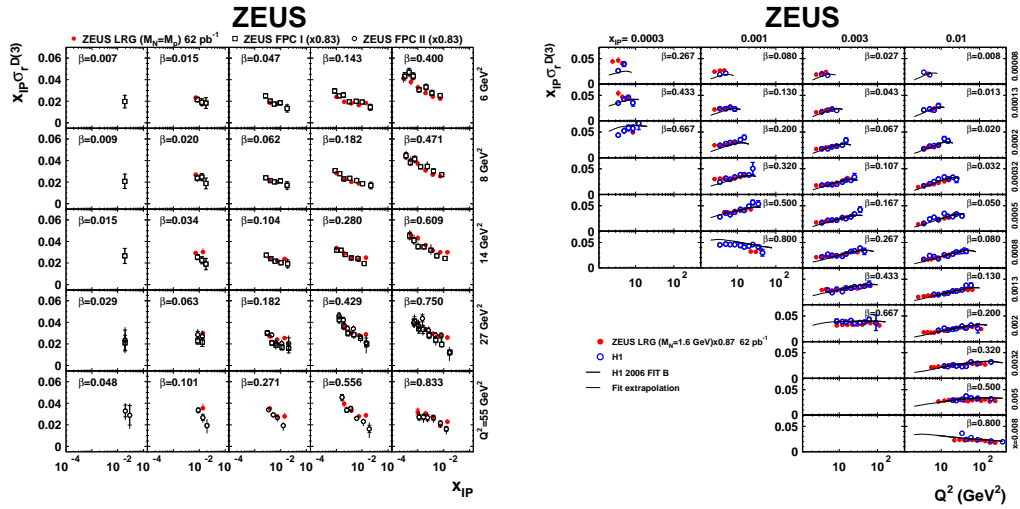


Figure 3: (left) Reduced diffractive cross section obtained by ZEUS with the LRG and M_X methods as a function of $x_{\mathbb{P}}$ for different values of Q^2 and β . (right) Reduced diffractive cross section obtained with the LRG method as a function of Q^2 for different values of $x_{\mathbb{P}}$ and β compared with the H1 results and with the H1 DPDF 2006 Fit B predictions, the ZEUS results are normalised to the H1 results.

carries an integrated fraction of $\sim 70\%$ of the momentum of the diffractive exchange.

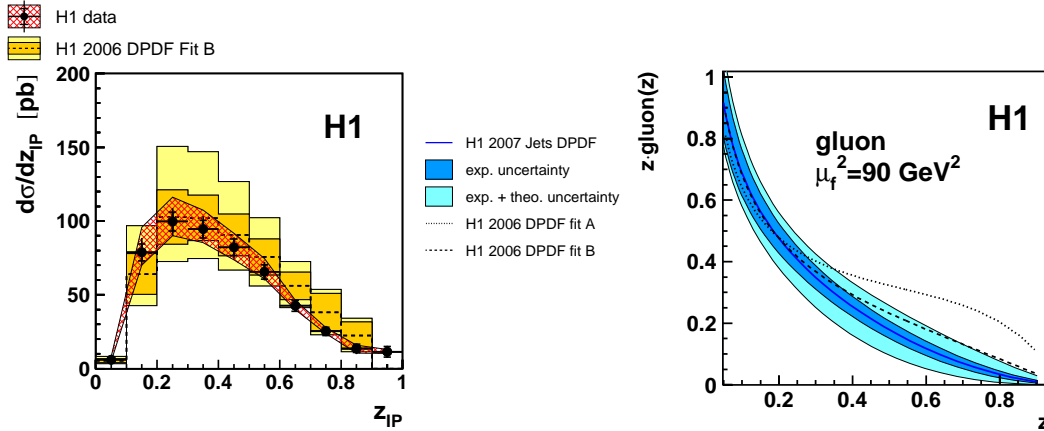


Figure 4: (left) Differential cross section of diffractive dijet production in DIS vs $z_{\mathbb{P}}$ compared with H1 2006 DPDF fit B. (right) Diffractive gluon density for a value of the hard scale of 90 GeV^2 . The solid line indicates the combined fit of the H1 inclusive and dijet DIS data, the dashed lines shows the results of the H1 2006 DPDF fit A and B to inclusive DIS data.

The H1 DPDF results has been used to predict the diffractive dijet cross sections in DIS [16]. This process is dominated by boson-gluon fusion, where a hard collision of a virtual photon and a gluon produces a high- p_T $q\bar{q}$ pair. Therefore, the diffractive dijet data are directly sensitive to the gluon content of the diffractive exchange.

Figure 4(left) shows the differential cross section for diffractive dijet production in DIS

as a function of $z_{\mathbb{P}}$, the fraction of the momentum of the diffractive exchange carried by the parton entering the hard scattering, compared to a prediction based on the H1 2006 DPDF Fit B. The $z_{\mathbb{P}}$ distribution is the most sensitive to the gluon DPDFs. The H1 2006 DPDF Fit B describes the diffractive dijet DIS cross section, whereas the Fit A overestimates the dijet data. The dijet data were used by H1 as an additional constrain for both quark singlet and gluon densities in the NLO QCD procedure. The new set of diffractive PDFs, the H1 2007 Jets DPDF, provides the most precise diffractive quark and gluon distributions in the range $0.05 < z_{IP} < 0.9$. The simultaneous fit of both the inclusive and dijet data provides big improvement in the precision of the gluon density at high fractional momentum compared to the previous extractions, fig. 4 (right).

In dijet photo-production (PhP) the hard scale is defined by E_T of jets because $Q^2 \sim 0$. QCD collinear factorization is expected to be valid in direct processes with pointlike photon, but broken in processes with resolved photons, where secondary interactions between photon and proton remnants fill the rapidity gap. These two processes can be separated using the variable x_γ , which corresponds to the longitudinal momentum fraction of the photon entering the hard sub-process. Resolved photon processes correspond to $x_\gamma < 1$, whereas direct photon processes to $x_\gamma \simeq 1$.

Neither H1 [25], nor ZEUS [24] observe a significant difference in the description of the data in the resolved (low x_γ) and direct (high x_γ) regions by NLO predictions based on QCD collinear factorization and DPDFs. The H1 Collaboration has also presented measurements in two ranges of E_T of jets and found that the suppression of the dijet data relative to NLO predictions is decreasing with increasing of E_T of jets (Fig. 5). The ZEUS results also confirm this tendency. The dijet photoproduction cross sections from H1 and ZEUS are found to be consistent within uncertainties when measured in the same E_T range, although the ratio of the H1 cross section to NLO predictions is somewhat lower than the ZEUS value.

2.2 Exclusive diffraction in ep interaction

The transition from purely soft to hard pQCD processes is studied at HERA in the vector meson (VM) production. In particular, it is expected that the VM production cross section increases with increasing photon-proton centre-of-mass energy as $\sim W^\delta$, with the power factor δ growing with Q^2 . Moreover, the effective size of the virtual photon decreases with Q^2 , leading to a flatter distribution in t . Both the features have been observed at HERA and presented at the conference.

In particular, H1 presented new results on the ρ and ϕ electro-production [26] and DVCS [21, 17]). ZEUS presented recently published results on the ρ -meson electro-production [22] and new results

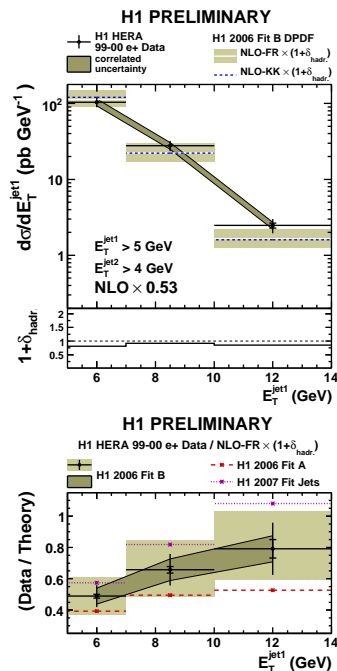


Figure 5: Differential cross section of the diffractive dijet photo-production as a function of E_T of the hardest jet. The data are compared to the NLO QCD predictions based on the H1 DPDF fits.

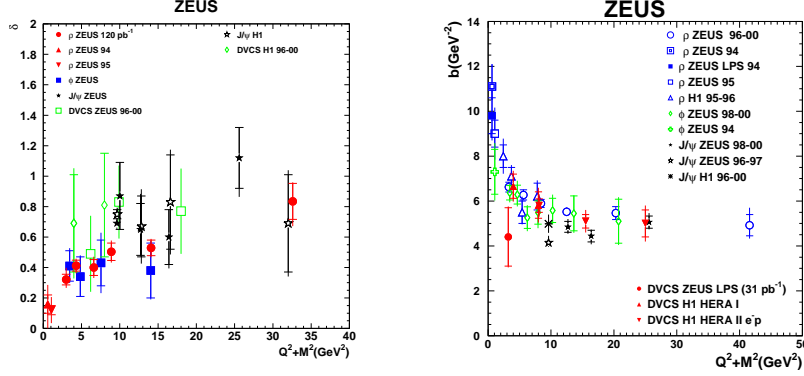


Figure 6: A compilation of the values of δ (left) and b (right) for exclusive VM electroproduction as a function of $Q^2 + M^2$ including the DVCS results.

on Υ in photoproduction and DVCS [23, 13].

The H1 and ZEUS results are summarized in Fig. 6. The left figure shows a compilation of the δ values as a function of the scale $Q^2 + M^2$ obtained for various VM and DVCS. It is found that δ increases with the scale for all VMs, as expected in pQCD. The right figure shows a compilation of the b values obtained from an exponential fit to the differential cross section as a function of the scale $Q^2 + M^2$ for various VMs and DVCS. The figure shows the transition from soft to hard regime with b decreasing with increasing scale up to the asymptotic value of 5 GeV^{-2} , as expected in pQCD.

The t -dependence of the DVCS cross section has been studied by ZEUS using a direct measurement of the variable t with a LP spectrometer. The measurement was performed in the kinematic region, $Q^2 > 1.5 \text{ GeV}^2$ and $40 < W < 170 \text{ GeV}$. The result is presented in the upper part of Fig. 7. In the DVCS analysis of H1 the variable t was computed as a vector sum of the transverse momenta of the final state photon and the scattered lepton. H1 studied the differential cross section as a function of t for different values of Q^2 and W . The lower part of Fig. 7 shows the b values obtained by H1 for different Q^2 values. A soft Q^2 dependence and no W -dependence of the parameter b was observed.

H1 also measured the ratio of the proton dissociative to elastic cross sections for ρ and ϕ

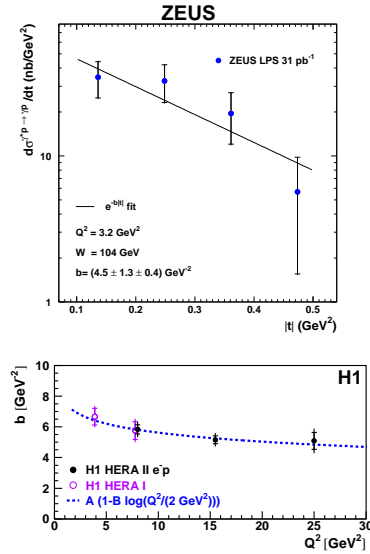


Figure 7: Differential cross section of DVCS measured by ZEUS as a function of t . The result of the fit with an exponential function is shown (upper). Parameter b of the DVCS t -distribution measured by H1 as a function of Q^2 (lower).

electroproduction [26]. The ratio is found to be independent of Q^2 . The result is consistent with the hypothesis of proton vertex factorisation. The Q^2 and t dependences of spin density matrix elements have been studied and the ratios of polarised amplitudes in ρ and ϕ electroproduction have been extracted confirming SCHC violation.

3 Results from the Tevatron and prospects at the LHC

Describing hard diffractive hadron-hadron collisions is more challenging than describing hard diffractive ep collisions since factorisation is broken by rescattering between spectator partons. These rescattering effects, often quantified in terms of the so-called ‘‘rapidity gap survival probability’’ [29], $\langle |S^2| \rangle$, are of interest in their own right because of their relation with multiple parton scattering. To first approximation, the cross section for diffractive hadron-hadron collisions is directly proportional to $\langle |S^2| \rangle$, independent of kinematics.

At the Tevatron, single diffraction cross sections for vector boson, di-jet and heavy quark production are observed that are lower by a factor $\mathcal{O}(10)$ relative to the theoretical predictions based on the diffractive PDFs from HERA. This translates into a ratio of diffractive to non-diffractive production at the Tevatron of $\sim 1\%$. Theoretical expectations at the LHC are at the level of a fraction of a per cent [30]. There are, however, significant uncertainties in the predictions, notably due to the uncertainty of $\langle |S^2| \rangle$. While there is some consensus that $\langle |S^2| \rangle \simeq 0.05$ [31], values between 0.004 and 0.23 have been proposed [32].

Interest in diffraction at the LHC has been greatly boosted recently by theoretical predictions [33] that identified central exclusive production (CEP) as a potential discovery channel for the Higgs boson. Experimental evidence from the Tevatron on CEP of di-jets, di-photons and di-leptons support the validity of the underlying theoretical model. In the last years, both ATLAS and CMS have set up forward physics programs. In addition, FP420, a joint R&D program of ATLAS, CMS and the LHC machine group has investigated the feasibility of an upgrade of the forward detector instrumentation to make possible the direct observation of the scattered protons in CEP of a Higgs boson.

3.1 Diffraction with a hard scale

The CDF experiment reported preliminary results [34] from their run-II data for the process $\bar{p}p \rightarrow pWX$ and $\bar{p}p \rightarrow pZX$. These processes are sensitive to the quark component of the diffractive PDFs. The run-II analysis employs the MiniPlug calorimeters ($3.5 < |\eta| < 5.5$) for E_T and angular measurements, Beam Shower Counters ($5.5 < |\eta| < 7.5$) to identify rapidity gaps and the CDF Roman Pot Spectrometer to detect leading \bar{p} with $0.03 < \xi < 0.09$, where ξ is the fractional momentum loss of the \bar{p} . A novel feature of the analysis is the determination of the full kinematics of the $W \rightarrow e\nu/\mu\nu$ decay by obtaining the neutrino E_T^ν from the missing E_T , as usual, and η_ν from the difference of the ξ measured by the Roman Pot detectors and the central calorimeter. The results for the ratio of single diffractive to non-diffractive production obtained from a data sample of 0.6 fb^{-1} are:

$$R_W(0.03 < \xi < 0.10, |t| < 0.1) = [0.97 \pm 0.05 \text{ (stat)} \pm 0.11 \text{ (syst)}]\%$$

$$R_Z(0.03 < \xi < 0.10, |t| < 0.1) = [0.85 \pm 0.20 \text{ (stat)} \pm 0.11 \text{ (syst)}]\%$$

These results are in good agreement with the run-I results from D0 and CDF after correcting for differences in acceptance to the rapidity-gap-based selection used then.

The CMS experiment studied the feasibility of observing single diffractive W production [35] with $W \rightarrow \mu\nu$ at LHC energies and for an effective integrated luminosity for single

interactions of 100 pb^{-1} . The selection is rapidity-gap based and requires the absence of activity in the forward calorimeters of CMS, i.e. in HF ($3 < |\eta| < 5$) and CASTOR ($-6.6 < \eta < -5.2$). At LHC start-up the latter will be available only on one side of the interaction point. Assuming a rapidity gap survival probability of 0.05, $\mathcal{O}(100)$ signal events are expected with a signal-to-background ratio as high as 20 if the CASTOR calorimeter is available.

3.2 Central exclusive production processes at the Tevatron

Central exclusive processes are of the type shown in Fig. 8. The p, \bar{p} emerge intact, with only a small momentum loss, while the interaction products are emitted into the central region. Processes of this type may provide a discovery channel for the Higgs boson at the LHC, as predicted by the KMR model [33]. Experimental evidence for the validity of this model can be gained from Tevatron data on CEP of di-jets and di-photons.

The CDF experiment presented final results for the CEP of di-jets [34], see Fig. 8. The data favor the KMR model, which is implemented in the Monte Carlo generator ExHuMe [36]. CDF also reported on evidence for the first observation at hadron colliders of CEP of di-photons [37]. Three candidate events were observed in 532 pb^{-1} of CDF run-II data, in agreement with ExHuMe predictions. Currently it cannot be excluded that some of the candidate events are $\pi^0\pi^0$ or $\eta\eta$ events, and further analysis is on-going.

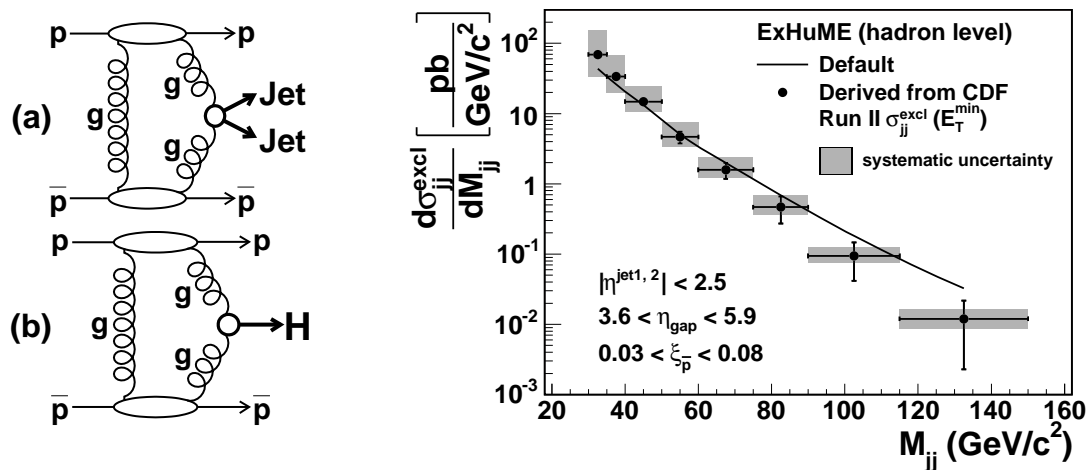


Figure 8: Diagrams for exclusive di-jet (a) and Higgs (b) production, and the ExHuMe [36] exclusive di-jet differential cross section at the hadron level vs. di-jet mass M_{jj} normalized to measured σ_{jj}^{excl} values. The solid curve is the cross section predicted by ExHuMe.

3.3 Exclusive dilepton and vector meson production

Production of exclusive dileptons, of the type $\bar{p}p \rightarrow \bar{p}l^+l^-p$, can occur in two-photon interactions, $\gamma\gamma \rightarrow l^+l^-$, and in vector meson photoproduction, $\gamma p \rightarrow Vp \rightarrow l^+l^-p$. The former process is to good approximation a pure QED process, with a cross section known to high precision. At the LHC it can be used for absolute luminosity determination. The latter

process gives access to the gluon content of the proton and has been studied at HERA for different types of vector mesons.

CDF reported previously the first observation of $\gamma\gamma \rightarrow e^+e^-$ production at a hadron collider [37]. Sixteen events were found in 532 pb^{-1} of CDF run-II data, where the electrons have a minimum E_T of 5 GeV and the exclusivity condition requires the absence of any particle signatures other than the electrons in the full η range covered by the CDF detector, i.e. down to $|\eta| = 7.5$. Background pollution was estimated to be 1.9 ± 0.3 events, dominated by events where the p or \bar{p} dissociates. A cross section of $1.6_{-0.3}^{+0.5}(\text{stat}) \pm 0.3(\text{syst.}) \text{ pb}$ was obtained, in good agreement with the prediction from the LPAIR Monte Carlo [38]. The search for exclusive di-muon production in CDF run-II data is on-going. CDF reported the observation, for the first time at a hadron collider, of J/ψ and ψ' photoproduction candidates [37]. The background from $\chi_c \rightarrow J/\psi + \gamma(\text{soft})$, where the soft photon is not detected, is under study. Search for Υ photoproduction is likewise under way.

Feasibility studies for exclusive dilepton and vector meson photoproduction were presented by CMS [40]. Assuming the cross section predictions of the LPAIR and STARLIGHT [39] Monte Carlo generators, $\mathcal{O}(700)$ events are expected for an effective integrated luminosity of single interactions of 100 pb^{-1} . The largest source of background ($\mathcal{O}(200)$) comes from p dissociative processes. The number of non-resonant dimuon events will be sufficient to calibrate the integrated luminosity to a precision of $\sim 4\%$. A significant signal for photoproduction of the first three Υ resonances will be visible. The mean value of the effective γp center of mass energy in these events is $\langle W \rangle \sim 2400 \text{ GeV}$ and hence an order of magnitude larger than for the measurements available from HERA. The cross section is sensitive to the generalised parton distribution function (GPD) for the gluons. The distribution of the four-momentum squared at the proton vertex, t , is sensitive to the two-dimensional distribution of the gluons in the transverse plane, and has never been measured before for the Υ . Although t cannot be measured directly with CMS, the measured p_T^2 distribution of the Υ can be used as effective estimator of the true t distribution.

Theoretical predictions in the color dipole model for the cross section of exclusive Υ photoproduction at Tevatron and LHC and for the Υ rapidity distribution were presented in [41]. An enduring open question in our understanding of color neutral gluonic exchanges in perturbative QCD is the absence of experimental evidence for the Odderon, the C -odd partner of the Pomeron. In [42], the sensitivity at Tevatron and LHC of the normalized differential cross-section $(d\sigma/dp_T^2)/\sigma$ for the exclusive photoproduction of J/ψ and Υ was discussed.

3.4 Central exclusive Higgs production

Interest in diffractive processes at the LHC was boosted in recent years by the realization that double-Pomeron exchange processes may in fact augment the Higgs discovery reach at the LHC or render possible a precise measurement of the mass and quantum numbers of the Higgs boson should it be discovered by traditional searches. This is the CEP process [33], $pp \rightarrow p + \phi + p$, where the plus sign denotes the absence of hadronic activity between the outgoing protons, which survive the interaction intact, and the state ϕ . The final state consists solely of the scattered protons, which may be detected in forward proton taggers, and the decay products of ϕ which can be detected in the central CMS detector. Selection rules force the produced state ϕ to have $J^{CP} = n^{++}$ with $n = 0, 2, \dots$. This process offers hence an experimentally very clean laboratory for the discovery of any particle with

these quantum numbers that couples strongly to gluons. Additional advantages are the possibility to determine the mass of the state ϕ with excellent resolution from the scattered protons alone, independent of its decay products, and the possibility, unique at the LHC, to determine the quantum numbers of ϕ directly from the azimuthal asymmetry between the scattered protons.

A detailed mapping of the discovery potential of CEP in the MSSM was presented in [43]. In particular CEP of the neutral CP -even Higgs bosons h and H and their decays into bottom quarks has the potential to probe interesting regions of the MSSM parameter space and give access to the bottom Yukawa couplings of the Higgs boson up to masses of $M_H \leq 250$ GeV. CEP may also give access to the NMSSM Higgs bosons, which would be unique at the LHC [44]. Early measurements at the LHC to check the validity of the CEP models for Higgs production were discussed in [45]. Forward proton tagging would also provide the possibility for precision studies of γp and $\gamma\gamma$ interactions at center-of-mass energies never reached before [46].

3.5 Status of forward physics projects at the LHC

Both ATLAS [49] and CMS [48] presented the status of their detectors that extend beyond the central detector volume ($|\eta| < 5$). Both experiments have Zero Degree Calorimeters with acceptance for neutral particles for $|\eta| > 8.3$. Apart from those, their forward instrumentation is quite complementary. ATLAS is equipped with a dedicated luminosity system consisting of ALFA, Roman-pot housed tracking detectors at 240 m from the interaction point (IP), which will perform an absolute luminosity measurement in runs with special LHC optics, and of LUCID, Cherenkov detectors ($5.6 < |\eta| < 6.0$) for the primary purpose of luminosity monitoring during routine LHC data taking. At the CMS IP, the task of an absolute luminosity determination will be carried out by an independent experiment, TOTEM, with Roman-pot housed silicon detectors at 220 m distance from the IP and two tracking telescopes inside of the CMS volume. CMS in addition has the CASTOR calorimeter which extends the CMS calorimetric coverage to rapidity values of 6.5. CASTOR gives access to the QCD parton evolution dynamics at very low x . HERA has explored low- x dynamics down to values of a few 10^{-5} . At the LHC the minimum accessible x decreases by a factor ~ 10 for each 2 units of rapidity. A process with a hard scale of $Q \sim 10$ GeV and within the acceptance of CASTOR ($\eta \sim 6$) can occur at x values as low as 10^{-6} .

In order to give access to CEP Higgs production proton taggers at distances larger than 220/240 m are necessary. The FP420 R&D collaboration over the last years has investigated the feasibility of instrumenting the region at 420 m from the ATLAS or CMS IP, within the cryogenic region of the LHC [47]. The FP420 R&D report was recently published [51]. It proposes a cryostat re-design to house the proton taggers which would employ 3-D silicon, an extremely radiation hard novel silicon technology. Additional fast timing Cherenkov detectors would be capable of determining, within a resolution of a few millimeters, whether the tagged proton came from the same vertex as the hard scatter visible in the central detector. The FP420 proposal is currently under scrutiny in both ATLAS and CMS. If approved, installation could proceed in 2010, after the LHC start-up.

3.6 Summary

Hadron collider experiments have provided a wealth of data on diffraction and vector meson production in the past, and will continue to do so in the future with the imminent start-up

of the LHC.

References

- [1] Slides:
<http://indico.cern.ch/contributionDisplay.py?contribId=8&sessionId=8&confId=24657>
- [2] P.D.B. Collins, *An Introduction to Regge Theory and High Energy Physics*, Cambridge University Press, Cambridge, 1977.
- [3] A. Donnachie, P.V. Landshoff, Phys. Lett. **B296** 227 (1992);
J. Cudell *et al.*, Phys. Rev. **D61** 034019 (2000); Erratum, Phys. Rev. **D63** 059901 (2001).
- [4] M. Arneodo, M. Diehl, *Diffraction for non-believers*, hep-ph/0511047 (2005)
- [5] L. Trentadue and G. Veneziano, Phys. Lett. **B323** 201 (1994);
J.C. Collins, Phys. Rev. **D57** 03051 (1998); Erratum, *ibid.* **D61** 019902 (2000);
A. Barrera and D.E.Soper, Phys. Rev. **D53** 06162 (1996).
- [6] H1 Coll., A. Aktas *et al.*, Eur. Phys. J. **C48** 715 (2006);
H. Abramowicz, Int. J. Mod. Phys. A **S1b**, 495 (2000).
- [7] H1 Coll., A. Aktas *et al.*, Eur. Phys. J. **C48** 749 (2006);
ZEUS Coll., S. Chekanov *et al.*, Eur. Phys. J. **C38** 43 (2004);
ZEUS Coll., S. Chekanov *et al.*, Eur. Phys. J. **C25** 169 (2002);
ZEUS Coll., J. Breitweg *et al.*, Eur. Phys. J. **C1** 81 (1997).
- [8] http://www-h1.desy.de/h1/www/publications/H1_sci_results.shtml, H1-prelim-06-014;
ZEUS Coll., S. Chekanov *et al.*, Eur. Phys. J. **C25** 169 (2002).
- [9] ZEUS Coll., S. Chekanov *et al.*, Nucl. Phys. **B713**, 3 (2005).
- [10] ZEUS Coll., S. Chekanov *et al.*, DESY-08-011, submitted to Nucl. Phys. **B**.
- [11] http://www-zeus.desy.de/public_results/groupsearch.php, ZEUS-pub-08-010.
- [12] G. Ingelman and P.E. Schlein, Phys. Lett. **B152** 256 (1985).
- [13] http://www-zeus.desy.de/public_results/groupsearch.php, ZEUS-pub-08-013.
- [14] H1 Coll., A. Aktas *et al.*, Eur. Phys. J. **C48** 715 (2006).
- [15] H1 Coll., A. Aktas *et al.*, Eur. Phys. J. **C48** 749 (2006).
- [16] H1 Coll., A. Aktas *et al.*, JHEP **0710** 042 (2007).
- [17] H1 Coll., A. Aktas *et al.*, Phys. Lett. **B659** 796 (2008).
- [18] M. Ruspa, these proceedings.
- [19] P. Newman, these proceedings.
- [20] P. Laycock, these proceedings.
- [21] L. Favart, these proceedings.
- [22] Justyna Ukleja, these proceedings.
- [23] J. T. Malka, these proceedings.
- [24] W. Slominski, these proceedings.
- [25] K. Cerny, these proceedings.
- [26] X. Janssen, these proceedings.
- [27] A. Levy, these proceedings.
- [28] L. Rinaldi, these proceedings.
- [29] J.D. Bjorken, Phys. Rev. D **47** (1993) 10111; A.B. Kaidalov *et al.*, Eur. Phys. J. C **21** (2001) 521
- [30] V.A. Khoze, A.D. Martin, M.G. Ryskin, Eur. Phys. J. C **55** (2008) 363
- [31] V.A. Khoze, A.D. Martin, M.G. Ryskin, Phys. Lett. B **643** (2006) 93; E. Gotsman, E. Levin, U. Maor, E. Naftali, A. Prygarin, hep-ph/0511060

- [32] J.S. Miller, Eur. Phys. J. C **56** (2008) 39
- [33] V. A. Khoze, A. D. Martin, M. G. Ryskin., Eur.Phys.J C19 (2001) 477, erratum C20 (2001) 599
- [34] K. Goulianos, these proceedings
- [35] A. Vilela Pereira, these proceedings
- [36] J. Monk, A. Pilkington, Comput. Phys. Commun. **175** (2006) 232
- [37] J. Pinfeld, these proceedings
- [38] J.A.M. Vermaseren, Nucl. Phys. B **229** (1983) 347
- [39] J. Nystrand, these proceedings
- [40] S. Olyn, these proceedings
- [41] G. Watt, these proceedings
- [42] L. Motyka, these proceedings
- [43] M. Tasevsky, these proceedings
- [44] J. Forshaw, these proceedings
- [45] V. Khoze, these proceedings
- [46] M. Van Der Donckt, these proceedings
- [47] B. Cox, these proceedings
- [48] P. Van Mechelen, these proceedings
- [49] A. Pilkington, these proceedings
- [50] O. Kepka, these proceedings
- [51] FP420 collab, M.G. Albrow et al., *The FP420 R&D Project: Higgs and New Physics with forward protons at the LHC*, arXiv:0806.0302 [hep-ex] (2008)